

SpaceInn

Work Package 3.3

Accompanying report on the deliverables
D3.10 due for 2016 June 30: interface query

M. Rainer and E. Poretti

INAF - Osservatorio Astronomico di Brera

June 28, 2016

1 Executive summary

The archive *Spectroscopic Indicators in a SeisMic Archive* (SISMA) has been successfully created in the framework of the SpaceInn project (Work Package 3.3).

SISMA contains both HARPS spectra and CoRoT light curves of 71 CoRoT asteroseismic targets, and additional HARPS spectra of other 190 variable stars observed in order to better characterize the variability classes of the CoRoT targets. In total there are 7103 spectra and 90 light curves (some CoRoT targets were observed in more than one run). The spectra were collected during two Large Programmes (LP 182.D-0356 and LP 185.D-0056) spanning over nine semesters, from December 2008 to January 2013.

The tasks performed to create the archive have been the following ones:

- the HARPS spectra have been reduced, normalized, and converted in VO-compliant FITS files. In particular, for each spectrum it was created or computed:
 - `*_full.fits`: the five columns reduced observed spectrum, with wavelength (barycentric corrected, in Å), reduced flux, normalized flux, signal-to-noise ratio and echelle order;
 - `*_nor.fits`: the automatically normalized spectrum, with the orders merged (wavelength and normalized flux only);
 - `*_mean.fits`: the LSD mean line profile;
 - the radial velocity and the projected rotational velocity $v \sin i$. In the case of double or multiple systems, these velocities have been computed, if possible, for all the components;
 - the ratio q_2/q_1 of the first two zero positions of the mean line profile Fourier transform, which is an indicator of differential rotation;
 - a CaHK activity index (useful for solar-like stars, less in the case of hotter stars with spectral type A or earlier);
 - V/R violet-to-red peak intensity ratio in the case of emission stars;
- the above values (radial velocities, $v \sin i$, q_2/q_1 , activity indices and V/R values) are written in the headers of the `*_full.fits`, `*_nor.fits`, and `*_mean.fits` files and in the `OBJECT_tbl.fits` file (a general overview of a star's spectroscopic time series);
- a binarity flag has been given to every target;
- the physical parameters T_{eff} , $\log g$, and $[\text{Fe}/\text{H}]$ have been computed for almost every target using the spectral synthesis software SME, and stored in the header of all the FITS files;
- for each star, a PDF file (`OBJECT_fit.pdf`) with the observed spectrum in the 5160-5190 Å region and the best-fit synthetic spectrum from SME is given (in the case of objects where the fit was not possible, `OBJECT_fit.pdf` shows only the observed spectrum);
- for each star, a PDF file (`OBJECT_profmed.pdf`) that allows a quick look at the pulsational content of the time series is given. In the case of objects where a single spectrum was observed, this coincides with the mean line profile of the spectrum;
- the CoRoT photometry of the 71 asteroseismic targets has been added to the archive;
- an user-friendly web interface has been created, so that the data can be easily be retrieved and viewed from the web address <http://sisma.brera.inaf.it>
- an article detailing all the work done in preparing the database has been submitted to A&A and attached to this report. The final version of the paper will probably be different due to the publication process.

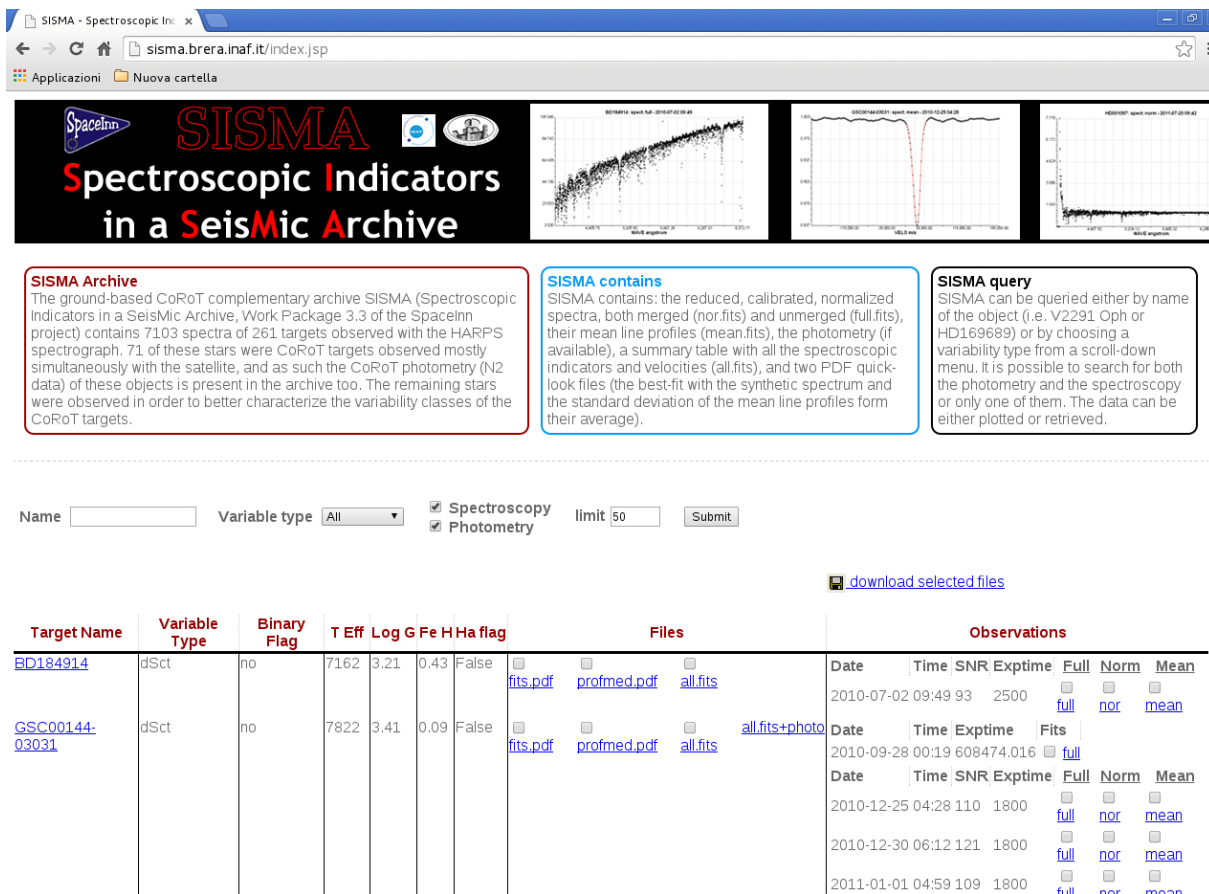


Figure 1: Web interface of the online archive SISMA. The archive can be found at <http://sisma.brera.inaf.it/>

As a result, the SISMA archive is now online and running. Figure 1 shows the web interface, that can be queried either by target name or by variability class. The results can be downloaded or plotted directly online. Because of the simultaneous ground-based and satellite's monitoring of the CoRoT targets, it is possible to overplot the light curves and the spectroscopic indicators of a star in order to study both photometric and spectroscopic variations.

The FP7-SPACE project *SpaceInn*: introducing SISMA, the HARPS archive of the asteroseismic CoRoT targets[★]

M. Rainer¹, E. Poretti¹, A. Mistò¹, R. Panzera¹, M. Molinaro², F. Cepparo², M. Roth³, E. Michel⁴, and M.J.P.F.G. Monteiro⁵

¹ INAF-Osservatorio Astronomico di Brera, via E. Bianchi 46, 23807 Merate, Italy
e-mail: monica.rainer@brera.inaf.it

² INAF-Osservatorio Astronomico di Trieste, via Tiepolo 11, 34143, Trieste, Italy

³ Kiepenheuer-Institut für Sonnenphysik, Schöneckstr. 6, 79104 Freiburg, Germany

⁴ Observatoire de Paris, LESIA, UMR8109, Université Pierre et Marie Curie, Université Paris Diderot, PSL, 5 pl. J. Jassen, 92195 Meudon, France

⁵ Instituto de Astrofísica e Ciências do Espaço, CAUP & DFA/FCUP, Universidade do Porto, Rua das Estrelas, 4150-762 Porto, Portugal

Received date / Accepted date

ABSTRACT

A large number of series of high-resolution spectra have been taken with different echelle spectrographs in order to complement the asteroseismic observations of the CoRoT satellite. In the framework of the EU FP7 collaborative project *SpaceInn: Exploitation of Space Data for Innovative Helio-and Asteroseismology*, 7103 spectra taken with the ESO echelle spectrograph HARPS have been stored in the VO-compliant database *Spectroscopic Indicators in a Seismic Archive* (SISMA), along with the CoRoT photometric data of the same objects. Several useful variability indicators (mean line profiles; indexes of differential rotation, activity and emission lines) together with $v \sin i$ and radial velocity measurements have been extracted from the spectra. The atmospheric parameters T_{eff} , $\log g$ and $[\text{Fe}/\text{H}]$ have been computed following a homogeneous procedure. The sample of 261 targets contained in the database aims at being a resource for in-depth studies of a wide range of variability classes.

Key words. Asteroseismology – Astronomical databases: miscellaneous – Line: profiles – Stars: fundamental parameters – Stars: variables: general

1. Introduction

The two main scientific programs of the *CO*nvection, *RO*tation and *planetary Transits* (CoRoT; Baglin et al. 2007) space mission focused on asteroseismological studies and extrasolar planets search. Each program used two dedicated CCDs and had different observational strategies: the asteroseismological program observed up to 5 stars brighter than magnitude $m_V=9$ per CCDs (10 in total) per observing run, while the exoplanet program observed around 6000 stars per CCD (12000 in total) of magnitude between 11 and 16. It was launched on December 27, 2006 and it was retired on June 24, 2013 after a second, unrecoverable electronic failure occurred on November 2, 2012. The first failure, in March 2009, caused the loss of two CCDs and the halving of the number of targets observed simultaneously.

The whole asteroseismic program was flanked by a large ground-based observational effort warranting a simultaneous monitoring (Poretti et al. 2007, 2013; Rainer et al. 2012; Uytterhoeven et al. 2009). Such a strategic decision was taken in the mission planning before launch in order to combine the high-quality photometry with simultaneous high-resolution spectroscopy. The asteroseismological strategy of the space mission CoRoT was to monitor several different types of pulsating and variable stars, in order to cover almost the whole

Hertzprung-Russell diagram. The observations were carried out on alternating short and long observing runs, of about 30 and 150 days respectively, focusing on up to 10 stars per run.

The ground-based activities started with the Large Programme 178.D-0361 using the FEROS spectrograph at the 2.2m telescope of the ESO-LaSilla Observatory, and continued with the Large Programmes LP182.D-0356 and LP185.D-0056 using the HARPS instrument at the 3.6m ESO telescope (Mayor et al. 2003). The spectroscopic survey branched out to several other high-resolution echelle spectrographs, i.e., SOPHIE at the Observatoire de Haute Provence, FOCES at Calar Alto Observatory, FIES and HERMES at the Roque de Los Muchachos Observatory, CORALIE at ESO-LaSilla Observatory, and HERCULES at the Mount John University Observatory.

The need to make available such a large archive of high-resolution spectra available to the whole community became urgent with the end of the CoRoT mission. Therefore, a specific activity was included in the EU FP7-SPACE collaborative project *SpaceInn: Exploitation of Space Data for Innovative Helio-and Asteroseismology*¹. Since HARPS was by far the most used instrument, first we focused on the 7135 spectra collected on 261 targets. Next activities, perhaps in other projects, could be the full reduction of the more diversified spectra collected with the other spectrographs. Thirty-two HARPS spectra have been discarded for quality reasons, and the remaining 7103

[★] This work is based on observations made with the 3.6-m telescope at La Silla Observatory under the ESO Large Programmes LP182.D-0356 and LP185.D-0056.

¹ <http://www.spaceinn.eu/>

have been stored in the web-based VO-compliant archive *Spectroscopic Indicators in a Seismic Archive* (SISMA), along with additional files and information. In this paper we illustrate the work done collecting the spectra, reducing them and obtaining the additional information stored in the archive (physical parameters, velocities, activity indices and so on), alongside the creation of the database.

2. Observations and reduction of the HARPS spectra

In the framework of the awarded two HARPS Large Programmes, we could observe 15 nights each semester over nine semesters, from December 2008 to January 2013, for a total of 135 nights of observations. We obtained high signal-to-noise ratio (S/N) spectroscopic time-series of a selection of the asteroseismological targets of CoRoT. We usually used HARPS in the high-efficiency mode EGGs, with resolving power $R=80,000$, since many of the CoRoT targets were hot stars, with large $v \sin i$ values, and this makes the high-accuracy mode HAM ($R=115,000$) ineffective in improving the radial velocity precision. We also note that the library of reference spectra used by the online reduction pipeline of HARPS does not include hot star templates, again lowering the precision of the radial velocity measurements for hot stars, even in the case of low $v \sin i$ values. Moreover, the EGGs mode allowed us also to reduce the exposure times, and to increase the S/N, which is very useful for the line-profile variations (LPVs) analysis. Nevertheless, some specific targets (cool, bright stars with low $v \sin i$) have been observed in the high-accuracy mode HAM ($R=115,000$), more appropriate for obtaining very precise radial velocity measurements for these cases.

Most of the spectra observed with EGGs have $S/N \sim 200$ at about 5800 \AA , while the HAM spectra usually have $S/N \sim 150$ in the same region. Figure 1 shows the distribution of the S/N values. In this plot the 1160 spectra obtained on HD 46375 are not reported. The intensive monitoring of this K-type star hosting an exoplanet with a short cadence (120 sec of maximum exposure time, $S/N \sim 50$) was aimed at detecting the solar-like oscillations in the radial velocity time series. Actually, this was a pilot study for the next Large Programme, that in principle should have covered the second extension of the CoRoT mission if it had not been halted by the final failure.

In addition to the primary targets, the satellite observed some specific asteroseismological targets in the exo CCDs, too. These objects are typically faint ($11 \leq m_V \leq 16$) and unsuitable for detailed spectroscopic studies. Nevertheless, we took a few spectra of some of them, in order to obtain the physical parameters (e.g., Poretti et al. 2011). As requested in the case of observations conducted in Visitor Mode, other objects were observed as back-up and filling targets, aiming at better defining the physical properties of the variability classes observed by CoRoT. The final spectral-type distribution of the targets is shown in Fig. 2.

All the HARPS spectra were reduced using a semi-automated pipeline developed at the Brera Observatory (Rainer 2003), which automatically normalizes the spectra and retain information on the wavelength range of the orders. The latter is very important for detailed spectroscopic analysis, because the S/N decreases greatly on the borders of the orders and the spectral lines in these regions may be distorted during the merging because of a lack of continuum on both sides of the lines. Our pipeline delivers two outputs for each spectrum: *a*) a five column

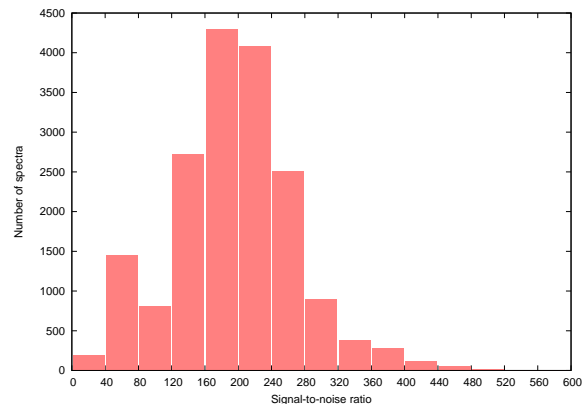


Fig. 1. Distribution of the signal-to-noise ratio of the observed spectra. The 1160 spectra of HD 46375 (S/N between 40 and 80) have been removed for easier reading.

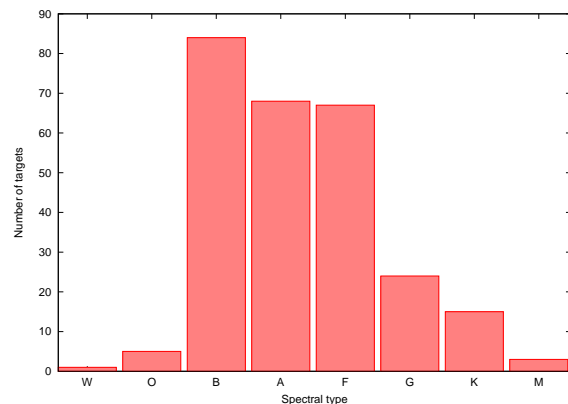


Fig. 2. Distribution of the spectral types of our targets.

table with wavelength, flux, normalized flux, S/N, and number of the echelle orders; *b*) a two-columns table with wavelength and normalized flux, with the echelle orders merged. The normalization was done in an automated way, as such the normalized spectra are to be used with care, keeping in mind that the normalization could be unreliable in the first orders and on the borders of the orders.

3. Data analysis: indicators

One or more papers have been published for almost every star in our sample, combining and discussing the spectroscopic and photometric time series (e.g., Poretti et al. 2009; Floquet et al. 2009; Mantegazza et al. 2012; Escorza et al. 2016). Still there is a lot of statistical work that can be done using our reduced spectra, and providing additional information on the objects will help in this endeavour. So we decided to estimate some useful indicators to be added to the archive. Because we wanted to support the asteroseismological exploitation of our data, we focused on

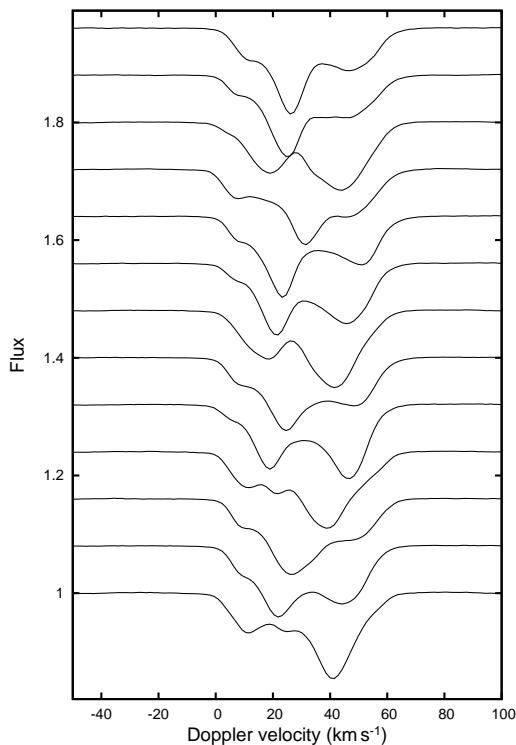


Fig. 3. Mean line profiles of the δ Scuti star HD 41641: the fluxes have been shifted for easier interpretation. The line-profile variations are greatly enhanced by averaging a great number of spectral lines.

results that will help the study of stellar variability, caused either by pulsations, rotational activity or emissions.

3.1. Mean line profiles: line-profile variations and rotational velocities

We computed the mean line profiles of each spectrum using the LSD software (Donati et al. 1997) on the wavelength regions 4415-4805, 4915-5285, 5365-6505 Å, i.e. we cut the beginning of the spectra, where usually the S/N is very low and the automated normalization procedure may fail, the end of the spectra, where most of the telluric lines are found, and the Balmer lines regions. We used a 0.8 km s^{-1} step for the HAM spectra and a 1.4 km s^{-1} step for the EGGs spectra, aside for some cases where we were forced to compute the mean line profiles in a very large velocity range (up to 1000 km s^{-1}) to take into account very fast rotation in binaries, and as such we increased the step up to 4 km s^{-1} for computational reasons. The mean line profiles are very useful to give clues of the importance of the nonradial oscillations. Figure 3 shows the clear perturbations due to a nonradial pressure mode in the mean line profiles of the δ Sct star HD 41641: the most probable identification of such mode is $(\ell, m) = (3, 1)$ (Escorza et al. 2016). The line-profile variations also provide the most stringent piece of evidence that high-degree ℓ modes ($\ell \geq 6$) are excited in δ Sct stars (see Fig. 8 in Poretti et al. 2009 and Fig. 13 in Mantegazza et al. 2012).

In order to provide a quick look at the pulsational content of the time series in the archive, we created for each target a

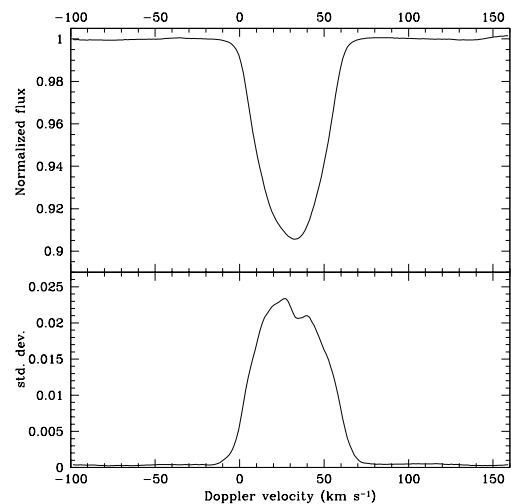


Fig. 4. Average mean line profile and standard deviations for A-type star HD 41641. The line-profile variations are clearly concentrated at the center of the line.

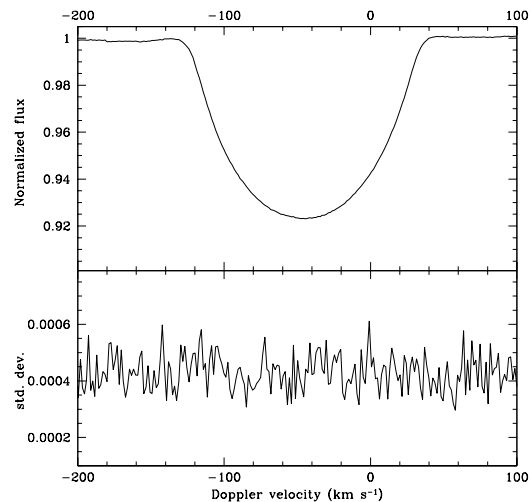


Fig. 5. Average mean line profile and standard deviations for A-type star HD 170133, where no line-profile variations are present.

PDF figure with the average of the mean line profiles of the spectra and their standard deviation from the average. Stars exhibiting line-profile variations clearly show a variable standard deviation along the average line profile, giving also hints where the deviations are the largest ones (see Fig. 4 again for the case of HD 41641). On the contrary, time series without line-profile variations show no variation. Figure 5 illustrates the clear constant behaviour of the line profiles of HD 170133, an A-type star found to be constant also in the CoRoT photometric time series.

We used the mean line profiles not only to measure the $v \sin i$ of the stars but, if possible, to indicate the presence of differential rotation, too. This is done using the Fourier transform of the symmetrized mean line profiles. The position of the first zero of the transform, q_1 , is used to compute the $v \sin i$ value. The q_2/q_1 ratio of the first two zero positions is an indication of possible solar-like differential rotation (if $q_2/q_1 < 1.72$), anti-solar differential rotation (if $q_2/q_1 > 1.83$), or rigid rotation

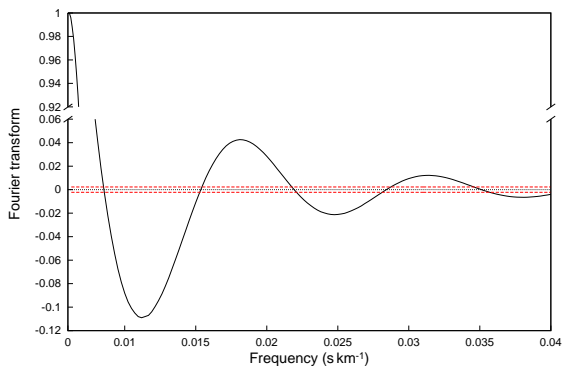


Fig. 6. Fourier transform of the mean line profile of a spectrum of HD 170133 (S/N=152). The red dashed lines show the very small region of uncertainty around the zero positions.

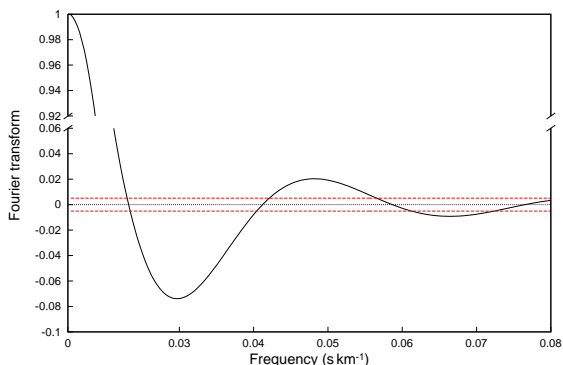


Fig. 7. Fourier transform of the mean line profile of a spectrum of HD 41641 (S/N=173). The red dashed lines show the region of uncertainty around the zero positions.

(if $1.72 < q_2/q_1 < 1.83$; Reiners & Schmitt 2002). This only works in case of rotators with $v \sin i > 10 \text{ km s}^{-1}$, where the rotation is the main contributor to the line broadening; otherwise we estimated the $v \sin i$ from the FWHM of the gaussian fitting of the mean line profiles and set the q_2/q_1 indicator as null. As an example, we obtained $v \sin i = 77.3 \pm 0.2 \text{ km s}^{-1}$ and $q_2/q_1 = 1.80 \pm 0.01$ for a spectrum of the non-variable star HD 170133 with S/N=152 (Fig. 6). The uncertainty on the zero position is very small due to the excellent mean line profile (Fig. 5). The situation is more complicated for the δ Sct variable HD 414641. Examining a spectrum with S/N=173, the effects of the pulsations on the mean line profiles resulted in much larger errors, i.e. $v \sin i = 29.8 \pm 2.2 \text{ km s}^{-1}$ and $q_2/q_1 = 1.76 \pm 0.26$ (Fig. 7). The indicators of differential rotation suggest rigid-body models for both stars.

We provided the radial velocities computed by the HARPS pipeline for the HAM spectra, while we computed those of the EGGs spectra by fitting the mean line profiles with a Gaussian.

Indeed, it was not possible to use the simultaneous lamp calibration in the EGGs mode because the dedicated fiber is broken. Moreover, most of our EGGs targets are hotter than the masks used by the ESO pipeline to compute the cross-correlation function: as such, the radial velocity computed by the HARPS pipeline is not as accurate as in the HAM mode.

3.2. Activity index

We decided to provide an indication of the stellar activity in order to better characterize the targets and to help study the stellar variations due to the pulsations along with activity variations. Because of the large range of spectral types, we defined a simple index using the H and K lines of Calcium (Rainer et al. 2006). Our index is not calibrated on the Mount Wilson one, since it is intended to be used to study variations only, not absolute values of activity.

To compute our activity index, we first re-normalized the region around the H and K lines, a task usually not well done by the automated procedure. Then we computed the areas of four spectral regions: two regions of 2.5 \AA each in the center of the H and K lines (A_H and A_K), and two regions of 10 \AA each on the continuum (A_{c1} and A_{c2}).

We obtained two indexes, one for the H line and one for the K line:

$$I_H = \frac{A_H}{(A_{c1} + A_{c2})/2} \quad I_K = \frac{A_K}{(A_{c1} + A_{c2})/2} \quad (1)$$

The final index is simply the average of the two individual ones:

$$I_{HK} = \frac{I_H + I_K}{2} = \frac{A_H + A_K}{A_{c1} + A_{c2}} \quad (2)$$

Values of I_{HK} larger than 0.2–0.3 indicate the presence of activity in the specific HARPS spectrum. The index is very useful to trace activity of solar-like stars, less for hotter star (spectral type A or earlier), but it is automatically computed and as such it is given for all the spectra. The activity index can be relied upon for more than one hundred stars of our sample.

3.3. Violet-to-red peak intensity ratio in Be stars

There are 40 stars in our archive that show emission lines. Mostly they are Be stars, i.e. stars from late O to early A spectral types surrounded by circumstellar disk fed by stellar mass loss outbursts: the emission lines of these stars are produced both by the stellar outbursts and by the disk.

Be stars show spectral and photometric variability on wide timescales, ranging from minutes to years; a interesting quantity to study is the violet-to-red peak-intensity ratio (V/R) which is the ratio between the peak intensity of the violet and the red part of the $H\alpha$ emission, and as such it is an indicator of the line asymmetry (Saad et al. 2012). Figure 8 shows the $H\alpha$ profile of the Be star HD 171219 (Andrade et al., in prep.). In most cases, Be stars have stable V/R equal to 1 (no asymmetry), but roughly a third of them show instead quasi-periodic V/R variations, which may be a combination of orbital period and long term variability (on a timescale of several years).

All the spectra in our archive have a true/false flag for the presence of emission in the $H\alpha$ line. In the case of emission, the value of V/R is given; if there is no emission, V/R is set to zero.

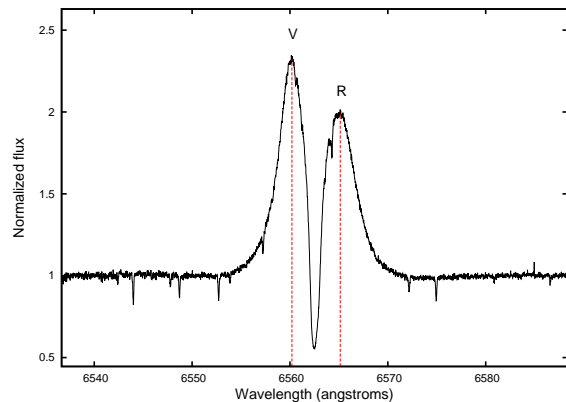


Fig. 8. Observed spectrum of the Be star HD 171219 in the $H\alpha$ region. The violet and red peaks of the emission are shown with dashed lines.

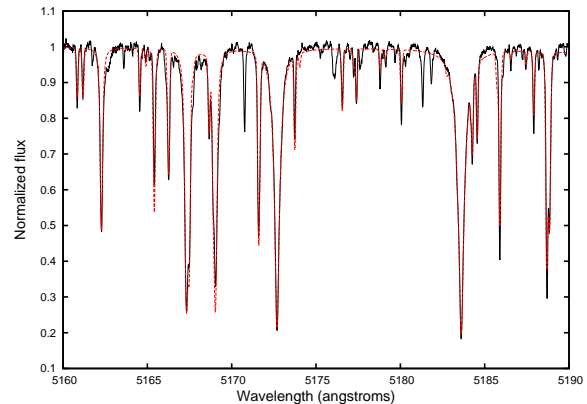


Fig. 9. Observed spectrum of the δ Scuti star HD 39996 (solid black line) and best synthetic fit (red dashed line).

4. Data analysis: physical parameters

The physical parameters of all the stars in the database are estimated with the spectral synthesis method using the 3.3 version of the SME software (Valenti & Piskunov 1996) and the stellar line lists from VALD (Piskunov et al. 1995) on a selected wavelength region (5160-5190 Å). We usually have several spectra for each star: in these cases we shifted the spectra by their measured radial velocities and then we averaged them, in order to lessen the effect of the pulsations on the shape of the stellar lines. Then we estimated the physical parameters (T_{eff} , $\log g$, and $[\text{Fe}/\text{H}]$) on the average spectrum.

Because the estimation of the errors on the parameters may be tricky, we provide for each star a PDF figure with the observed spectrum and the best fit (Fig. 9). For solar-like stars, the typical errors (*cgs* units) are of about 44°K in T_{eff} , 0.03 dex in $[\text{Fe}/\text{H}]$ and 0.06 dex in $\log g$ (Valenti & Fischer 2005), while for hotter, faster rotating stars they are larger (Tsantaki et al. 2014). In the case of very fast rotators, such as B-type stars, the resulting parameters are uncertain due to line blending and dilution in the continuum.

Under very special circumstances (e.g., very fast rotators, emission line stars, binary stars, and so on), we were not able to estimate the physical parameters with this automated method, as for example in the specific case of the strong emission lines of the Be star HD 128293 (Fig. 10). In these cases, a PDF figure with only the observed spectrum in the 5160-5190 Å region is given in the archive.

An online table is available in the App. A with the estimated physical parameters and other information (variability type, binarity, and so on): a sample can be seen in Tab. 1. The table provides the following information: Column 1 gives the name of the object, Column 2 the number of observed HARPS spectra, Column 3 the estimated T_{eff} , Column 4 the estimated $\log g$, Column 5 the metallicity $[\text{Fe}/\text{H}]$, Column 6 indicates the binarity, Column 7 gives the variability type of the object, Column 8 flags the presence of $H\alpha$ emission.

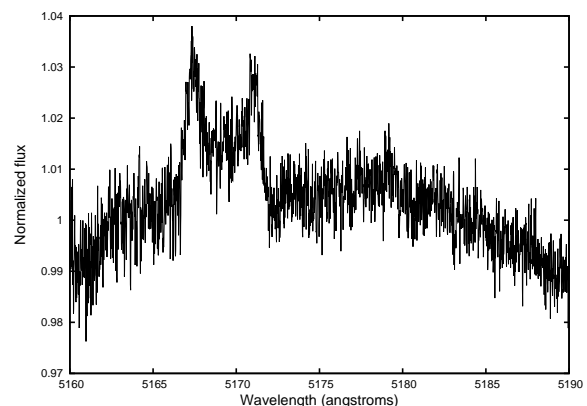


Fig. 10. Observed spectrum of the Be star HD 128293 in the 5160-5190 Å region. The emissions are clearly visible. It is not possible to fit this spectrum in order to estimate the physical parameters of the star.

Table 1. A sample of the table provided in the online App. A.

Target	N. sp.	T_{eff}	$\log g$	$[\text{Fe}/\text{H}]$	Bin.	Var. type	$H\alpha$ em.
BD184914	1	7162	3.21	0.43	no	dSct	no
HD001097	1	6595	3.70	0.31	no	dSct	no
HD007312	1	8378	3.88	0.55	no	dSct	no
HD008781	1	7280	2.91	-0.23	no	dSct	no
HD009065	35	7471	3.30	-0.41	no	dSct	no
HD009133	1	8812	4.25	0.49	no	dSct	no
HD010167	1	SB2	gDor	no
HD011462	10	11891	4.05	0.07	no	bCep	no
HD011956	1	8986	3.93	0.71	no	dSct	no
HD016031	14	5633	4.38	0.13	no	none	no
HD016189	65	7338	3.72	0.00	no	dSct	no
...

5. CoRoT photometry

The most observed stars, i.e. those with more spectra in the archive, are the main asteroseismological targets of the CoRoT Long Runs. In fact, the ground-based campaigns were planned to have the spectroscopic counterpart of the CoRoT light curve. The light curves of these 71 stars have been retrieved from the CoRoT public archive and stored in our database alongside the spectra. In some cases, the targets were observed with CoRoT in more than a Long Run resulting in more than one set of photometric data per target.

The CoRoT data are the N2 version². The reduction of the CoRoT data followed these steps:

- the N0 data are the time-stamped raw data produced at the CoRoT Mission Center (CNES), and they are not available outside of the CoRoT Mission or Data Center;
- the N1 data are corrected from instrumental effects only at the first order, and they were mostly used for alarm mode and instrument check;
- the N2 data are the main output of the CoRoT mission: they consist of the corrected light curves and they become public one year after their processing.

The N2 light curves are provided as FITS files, with some auxiliary information stored in the header. The FITS files contain three tables: N1 data, N2 data in the heliocentric frame with irregular time sampling, and N2 data in the heliocentric frame with regular 32 seconds sampling. Any new release of the CoRoT light curves will be added to the archive as soon as it will be made public.

The nights with HARPS were scheduled during the period of best visibility of the CoRoT targets and usually we were able to get the requested simultaneous spectroscopy and photometry. However, the time baseline of the spectroscopic observations is much smaller than that of the photometric ones (typically 20-25 nights against 30-150 days). Nevertheless, it was possible to monitor the spectroscopic counterpart of the photometric variations: Figure 11 shows an example of simultaneous radial velocity and flux measurements.

6. Structure of the spectroscopic Archive

All the data (reduced spectra, indicators and photometric series) are stored as either FITS or PDF files in the SISMA archive and can be accessed at <http://sisma.brera.inaf.it/>. The data can also be accessed through the Seismic Plus portal³. The portal was developed in the framework of the *SpaceInn* project in order to gather and help coordinated access to several different solar and stellar seismic data sources.

6.1. Database infrastructure

The operating system for the online archive (database and web pages) is Linux assembled under the model of free and open-source software development and distribution. The object-relational database management system (ORDBMS) is PostgreSQL, a free and open-source software developed by the PostgreSQL Global Development Group. The ORDBMS manages all data and files stored in the archive.

² <http://idoc-corot.ias.u-psud.fr/jsp/doc/DescriptionN2v1.3.pdf>

³ <http://voparis-spaceinn.obspm.fr/seismic-plus/>

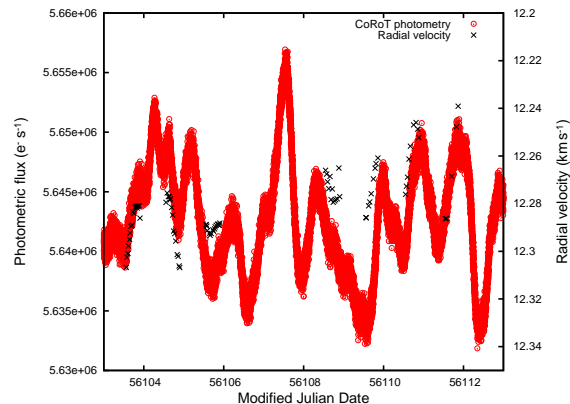


Fig. 11. Zoom of the simultaneous plot of the CoRoT light curve (red dots) and the radial velocity curve (black crosses) of the red giant HD 178484. Instead of the radial velocities, it is possible to plot any of the other spectroscopic indicators, i.e. $v \sin i$, q_2/q_1 , activity indices or V/R values.

The web user interface to the database is programmed using the Java/Servlet/JSP language, that creates web-based applications using Model View Controller. The web pages are Java Server Pages (JSPs) with embedded Java, HTML and CSS codes. The codes are executed on the server, then the page is returned to the browser for display. The server for Java Servlet and JSPs technologies is Apache Tomcat.

JSPs use RGraph⁴ for charts visualization, a JavaScript charts library that produces the charts dynamically with JavaScript and the HTML canvas tag. The charts are made inside the browser with JavaScript so they are both quick to create and small. The archive can be queried either by target (using the name resolver service Sesame⁵) or by variability class, and the data can be retrieved or displayed (Fig. 12). In the latter case, it is possible to plot the spectra, the light curves and the spectroscopic time series online. The library used to read the FITS files is STIL (Starlink Tables Infrastructure Library)⁶.

6.2. Scientific data

The database contains several files for each observed object:

- *_full.fits: the main deliverables, i.e., the reduced spectra. The five columns list wavelength (barycentric corrected, in Å), reduced flux, normalized flux, signal-to-noise ratio, and echelle order;
- *_nor.fits: additional reduced spectra, automatically normalized and with the orders merged. They have two columns (barycentric corrected wavelength in Å, and normalized flux). It is important to keep in mind that the normalization is done by an automated procedure and as such a careful check is necessary for a detailed study of any particular line;
- *_mean.fits: the mean line profiles of each spectrum computed with the LSD software in the 4415-4805, 4915-5285, 5365-6505 Å wavelength ranges. The files consist of two columns: Doppler velocity and normalized flux;

⁴ <http://www.rgraph.net/>

⁵ <http://cdsweb.u-strasbg.fr/doc/sesame.htm>

⁶ <http://www.star.bristol.ac.uk/~mbt/stil/>

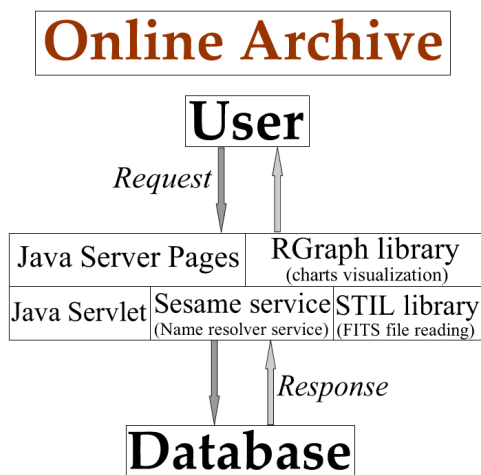


Fig. 12. The software used in the interaction between user and database.

- OBJECT_tbl.fits: a general overview of the object time series:
 - the root names of the spectra,
 - the barycentric Julian dates at mid-exposure,
 - the signal-to-noise ratios of the spectra in the 5805-5825 Å region,
 - the radial velocities of the spectra and their errors,
 - the projected rotational velocities $v \sin i$ of the spectra and their errors,
 - the q_2/q_1 values and their errors,
 - the activity index I_H , using only the Ca H line, of each spectrum,
 - the activity index I_K , using only the Ca K line, of each spectrum,
 - the averaged activity index I_{HK} of each spectrum,
 - the H α violet-to-red peak-intensity ratio (V/R) of each spectrum,
 - in the case of double or multiple systems, the radial velocities, $v \sin i$ and their errors will be listed for all the components, if possible;
- OBJECT_profmed.pdf: a PDF file that allows a quick look at the line-profile variations of the time series. In the case of objects where a single spectrum was observed, the mean line profile of the spectrum is given instead;
- OBJECT_fit.pdf: a PDF file with the observed spectrum in the 5160-5190 Å region and the best-fit synthetic spectrum. In the case of objects where the fit was not possible, only the observed spectrum is given.
- CoRoT light curves: FITS files with the CoRoT photometry. Light curves are available only for the 71 CoRoT targets having at least one HARPS spectrum.

Figure 13 summarizes how the data have been stored in the archive and how we structured the output of our reduction and analysis. Note that parameters and indices are properly stored in the FITS headers of the reduced spectra.

7. Conclusions

With the large number of space mission and ground-based campaigns that are continuously carried on, it becomes important to store the large amount of observational data in an easily accessible database, so that it can be exploited by the whole scientific

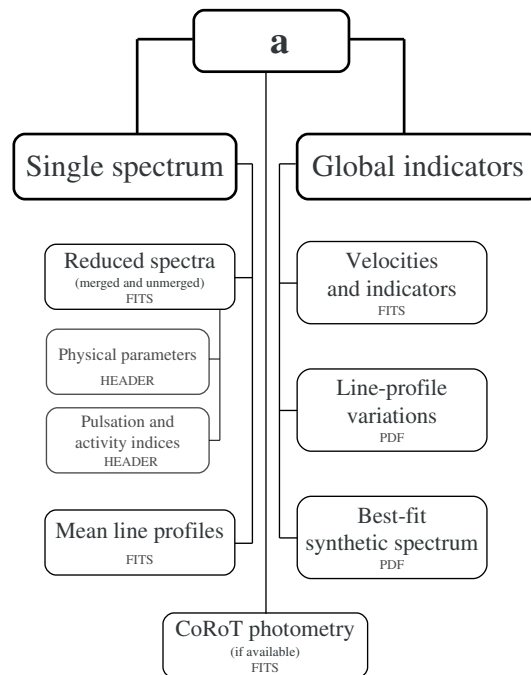


Fig. 13. Structure of the HARPS archive, with the content and format of the available files.

community. To this end, the *SpaceInn* project aims at coordinating several archives of helio- and asteroseismological data.

Towards this goal, we built the online database SISMA using the high-resolution HARPS spectra observed simultaneously with the CoRoT satellite, and the relative light curves. The reduced archived spectra are enriched with many observational parameters to be used as tools to investigate the spectroscopical effects of the stellar variability: mean line profiles, differential rotation indicators, activity indices, H α violet-to-red peak-intensity ratio along with the computed $v \sin i$ and radial velocity values. Stellar atmospheric parameters are also computed in a very homogenous way. All these data allow to study the stellar variations from several different angles. The spectra themselves are very useful for scientific purposes, being high S/N, high resolution, fully reduced and calibrated ones.

The ground-based spectra played a key role in the exploitation of the CoRoT mission thanks to the coordinated starting of the spectroscopic and photometric campaigns. Now we hope that the CoRoT ground-based complementary archive, with their high quality pre-processed spectra, could encourage more in-depth and statistical investigations on the stellar variability.

Acknowledgements. The research leading to this result has received funding from the European Community's Seventh Framework Programme (FP7/2007-2013) under grant agreement no. 312844. The authors thank Artie Hatzes for useful comments on a first draft of the manuscript.

References

- Baglin, A., Auvergne, M., Barge, P., et al. 2007, AIPC, 895, 201
- Donati, J.-F., Semel, M., Carter, B.D., Rees, D.E., & Collier Cameron, A. 1997, MNRAS, 291, 658
- Escorza, A., Zwintz, K., Tkachenko, A., et al. 2016, A&A, 588, A71
- Floquet, M., Hubert, A.-M., Huat, A.L., et al. 2009, A&A, 506, 103

- Mantegazza, L., Poretti, E., Michel, E., et al. 2012, *A&A*, 542, A24
Mayor, M., Pepe, F., Queloz, D., et al. 2003, *The Messenger*, 114, 20
Piskunov, N., Kupka, F., Ryabchikova, T.A., Weiss, W.W., & Jeffery, C.S. 1995, *A&AS*, 112, 525
Poretti, E., Michel, E., Garrido, R., et al. 2009, *A&A*, 506, 85
Poretti, E., Rainer, M., Uytterhoeven, K., et al. 2007, *MmSAIt*, 78, 624
Poretti, E., Rainer, M., Weiss, W.W., et al. 2011, *A&A*, 528, 147
Poretti, E., Rainer, M., Mantegazza, L., et al. 2013, *ASSP*, 31, 39
Rainer, M. 2003, Laurea Thesis (in italian), Università degli Studi di Milano
Rainer, M., Bossi, M., & Mantegazza, L. 2006, *ASPC*, 349, 319
Rainer, M., Poretti, E., Mathias, P., et al. 2012, *AN*, 333, 1061
Reiners, A., & Schmitt J.H.M.M., 2002, *A&A*, 384, 155
Saad, S.M., Hamdy, M.A., & Abolazm, M.S. 2012, *JAsGe*, 1, 97
Tsantaki, M., Sousa, S.G., Santos, N.C., et al. 2014, *A&A*, 570, 80
Uytterhoeven, K., Poretti, E., Mathias, P., et al. 2009, *AIPC*, 1170, 327
Valenti, J.A., & Piskunov, N. 1996, *A&AS*, 118, 595
Valenti, J.A., & Fischer, D.A. 2005, *ApJS*, 159, 141

Appendix A: Parameters table**Table A.1.** Physical parameters of the SISMA stars and additional information.

Target name	N. spectra	T_{eff}	$\log g$	[Fe/H]	Binary	Variable type	H α emission
BD184914	1	7162	3.21	0.43	no	dSct	no
GSC00144-03031	3	7822	3.41	0.09	no	dSct	no
HD001097	1	6595	3.70	0.31	no	dSct	no
HD007312	1	8378	3.88	0.55	no	dSct	no
HD008781	1	7280	2.91	-0.23	no	dSct	no
HD009065	35	7471	3.30	-0.41	no	dSct	no
HD009133	1	8812	4.25	0.49	no	dSct	no
HD010167	1	SB2	gDor	no
HD011462	10	11891	4.05	0.07	no	bCep	no
HD011956	1	8986	3.93	0.71	no	dSct	no
HD016031	14	5633	4.38	0.13	no	no	no
HD016189	65	7338	3.72	0.00	no	dSct	no
HD016698	1	7353	3.19	-0.38	no	dSct	no
HD017978	1	9058	4.58	0.43	no	dSct	no
HD021190	1	7804	3.44	0.41	no	dSct	no
HD022541	1	5976	1.53	-2.58	no	dSct	no
HD025637	1	6020	4.44	-0.52	no	dSct	no
HD026892	1	6979	3.00	0.37	no	dSct	no
HD027503	1	9884	4.86	0.85	no	dSct	no
HD027545	1	8009	3.62	0.40	no	dSct	no
HD028665	1	7559	3.05	0.58	no	dSct	no
HD028837	2	6964	2.74	0.33	no	dSct	no
HD030600	1	8072	3.46	0.27	no	dSct	no
HD030716	1	7029	2.87	0.35	no	dSct	no
HD031908	1	7458	3.04	0.22	no	dSct	no
HD032846	8	8045	3.69	0.24	SB2	dSct	no
HD033331	5	no	a2CVn	no
HD034816	112	no	none	no
HD039244	2	9457	4.00	0.78	no	dSct	no
HD039996	1	7451	4.25	0.49	no	dSct	no
HD040494	5	no	SPB	no
HD040726	2	5694	3.07	0.55	no	red-giant	no
HD041641	222	7561	3.71	0.06	no	dSct	no
HD041814	1	16043	2.81	-0.04	no	SPB	no
HD042089	1	6497	4.68	1.22	no	solar-like	no
HD042299	15	7871	4.05	0.10	no	dSct	no
HD042597	28	no	bCep	no
HD042618	3	5799	4.57	0.20	no	solar-like	no
HD042787	1	no	red-giant	no
HD042911	1	5393	3.40	0.55	no	red-giant	no
HD043023	1	5488	3.48	0.42	no	red-giant	no
HD043285	114	15890	3.72	-0.70	no	Be	yes
HD043317	191	no	SPB-bCep	no
HD043338	58	9518	4.56	1.03	no	gDor	no
HD043587	3	6021	4.59	0.37	SB1	solar-like	no
HD043823	1	6456	0.67	-0.52	no	none	no
HD043913	21	10945	3.32	-0.61	no	Be	yes
HD044195	387	8312	4.19	0.45	no	dSct-gDor	no
HD044958	1	9009	4.49	0.69	no	dSct	no
HD045398	104	4720	3.30	0.44	no	red-giant	no
HD045418	136	SB2	none	no
HD045517	1	8917	4.00	0.83	no	none	no
HD045546	141	21836	4.73	-0.10	no	bCep	no
HD045975	77	12564	4.03	0.11	SB1	HgMn	no
HD046149	37	SB2	none	no
HD046150	29	no	none	no
HD046202	58	no	bCep	no
HD046223	28	no	none	no

Table A.1. continued.

Target name	N. spectra	T_{eff}	$\log g$	[Fe/H]	Binary	Variable type	H α emission
HD046375	1160	5322	3.97	0.36	no	solar-like	no
HD046769	62	12048	3.38	-0.72	no	none	no
HD048752	1	no	none	no
HD048784	1	8324	3.71	0.57	no	dSct	no
HD048977	1	16484	3.92	-0.50	no	SPB	no
HD049310	3	no	none	no
HD049385	1	6438	4.16	0.45	no	solar-like	no
HD049429	1	5537	3.52	0.32	no	red-giant	no
HD049566	2	5570	3.45	0.39	no	red-giant	no
HD049585	17	no	Be	yes
HD049608	1	6025	2.93	0.64	no	red-giant	no
HD050230	4	SB2	SPB-bCep	no
HD050870	221	SB2	dSct	no
HD050890	5	5456	3.01	0.74	no	red-giant	no
HD051193	105	no	Be	yes
HD051452	106	no	Be	yes
HD051756	15	SB2	none	no
HD051844	4	6912	2.65	0.23	no	dSct	no
HD067523	360	7068	3.20	0.54	no	dSct	no
HD069213	104	7369	3.05	0.11	no	dSct	no
HD073654	1	no	SPB	no
HD075202	5	9209	4.46	0.68	no	RRLyr	no
HD075654	1	7772	3.94	-0.69	no	dSct	no
HD078422	1	7712	3.32	-0.11	no	dSct	no
HD079039	1	no	SPB	no
HD079185	1	6533	2.49	-0.50	no	dSct	no
HD079416	4	12728	3.54	1.00	no	SPB	no
HD080859	5	SB2	SPB	no
HD083041	1	8182	2.85	-0.04	SB2	dSct	no
HD083297	5	12509	3.69	0.19	no	SPB	no
HD084712	1	8238	3.74	0.46	no	dSct	no
HD084809	6	no	SPB	no
HD085012	5	no	SPB	no
HD085693	7	SB2	gDor	no
HD086659	7	SB2	SPB	no
HD087203	1	no	Be	yes
HD087700	1	8579	4.08	0.63	no	dSct	no
HD088263	1	no	Be	yes
HD089449	1	6358	4.10	0.32	no	dSct	no
HD090001	1	7059	3.52	0.14	no	dSct	no
HD090386	1	8560	3.01	0.95	no	dSct	no
HD090872	4	no	SPB	no
HD091024	41	no	aCyg	yes
HD091201	5	7161	3.70	0.34	no	gDor	no
HD093142	1	8769	4.04	0.60	no	dSct	no
HD093298	1	8328	1.50	0.18	no	dSct	no
HD094985	1	8015	1.51	-0.20	no	dSct	no
HD095321	1	11058	4.47	1.52	no	dSct	no
HD100363	1	SB2	dSct	no
HD101696	1	7869	3.64	0.07	no	dSct	no
HD103257	5	8328	4.41	0.41	no	gDor	no
HD104036	3	8386	4.14	0.23	no	dSct	no
HD105234	2	8544	4.46	0.43	no	dSct	no
HD105513	1	6877	3.00	-0.68	no	dSct	no
HD105521	1	no	Be	yes
HD109799	1	7340	3.72	0.40	no	gDor	no
HD110014	104	4988	3.42	0.63	SB1	no	no
HD110606	7	SB2	gDor	no
HD112091	1	no	Be	yes
HD112409	3	SB2	SPB	no
HD112999	1	no	Be	yes

Table A.1. continued.

Target name	N. spectra	T_{eff}	$\log g$	[Fe/H]	Binary	Variable type	H α emission
HD113357	7	7377	4.08	0.21	no	gDor	no
HD113537	1	6863	2.95	0.18	no	dSct	no
HD114042	2	9370	3.91	0.66	no	dSct	no
HD114620	1	7565	3.44	0.22	no	dSct	no
HD114839	2	8526	4.22	0.83	no	dSct	no
HD114981	1	no	Be	yes
HD116994	1	8022	3.94	-0.14	no	dSct	no
HD118285	5	SB2	SPB	no
HD120324	1	no	Be	yes
HD120500	1	10190	4.96	0.52	no	dSct	no
HD121190	6	no	SPB	no
HD124834	1	no	Be	yes
HD125081	1	7002	3.25	-0.06	no	dSct	no
HD126516	5	6652	4.01	0.02	SB1	gDor	no
HD126859	2	9840	4.49	1.17	no	dSct	no
HD127269	1	8964	4.27	0.58	no	dSct	no
HD128293	1	no	Be	yes
HD129041	1	9003	4.13	0.81	no	dSct	no
HD129231	1	9116	4.46	0.17	no	dSct	no
HD129954	1	no	Be	yes
HD131058	6	no	SPB	no
HD131168	1	no	Be	yes
HD131492	1	no	Be	yes
HD131976	113	3428	3.00	-1.74	SB1	none	no
HD132200	1	no	SPB	no
HD133738	2	no	Be	yes
HD133803	5	8610	4.76	0.44	no	gDor	no
HD135240	92	SB2	EB	no
HD135734	1	no	Be	yes
HD136415J	1	SB1	none	no
HD136504	28	SB2	bCep	no
HD137518	3	SB2	Be	yes
HD137785	6	8572	4.41	0.46	SB1	gDor	no
HD137949	10	no	a2CVn	no
HD138521	2	10444	2.77	0.24	no	SPB	no
HD142994	1	8602	3.07	0.03	no	dSct	no
HD143232	1	7550	3.37	0.28	no	dSct	no
HD143448	1	no	Be	yes
HD143578	3	no	Be	yes
HD144277	18	8660	4.26	-0.67	no	dSct	no
HD144965	1	no	Be	yes
HD146233	230	5760	4.35	0.05	no	solar-like	no
HD146444	2	no	Be	yes
HD146501	1	no	Be	yes
HD146596	1	no	Be	yes
HD147302	1	no	Be	yes
HD148259	3	no	Be	yes
HD148542	20	9316	2.87	0.60	no	a2CVn	no
HD149989	6	8679	4.74	0.24	no	gDor	no
HD150093	1	no	Be	yes
HD151113	1	no	Be	yes
HD151890	3	SB2	EB	no
HD152236	3	27875	3.62	0.01	no	sDor	yes
HD152478	1	no	Be	yes
HD152565	4	no	SPB	no
HD152635	2	no	SPB	no
HD153580	1	6451	4.32	0.04	SB2	gDor	no
HD153747	1	10749	5.34	0.12	no	dSct	no
HD154218	1	no	Be	no
HD155851	1	no	Be	yes
HD155854	6	SB2	gDor	no

Table A.1. continued.

Target name	N. spectra	T_{eff}	$\log g$	[Fe/H]	Binary	Variable type	H α emission
HD156325	1	no	Be	yes
HD156398	1	no	none	yes
HD158408	3	SB2	none	no
HD161032	1	7467	3.80	0.33	no	dSct	no
HD163899	3	23961	3.10	0.05	no	SPB	no
HD169370	1	5091	3.61	0.33	no	red-giant	no
HD169392A	2	6253	4.07	0.27	SB1	solar-like	no
HD169392B	2	6044	4.54	0.27	SB1	solar-like	no
HD169556	1	6302	4.47	0.86	no	solar-like	no
HD169689	155	5969	3.01	0.88	SB1	none	no
HD169751	1	5517	3.60	0.41	no	red-giant	no
HD169822	110	5700	4.60	0.19	no	none	no
HD170008	1	5495	3.97	0.00	no	red-giant	no
HD170031	111	5201	3.76	0.50	no	red-giant	no
HD170053	102	4899	3.03	0.29	no	red-giant	no
HD170133	32	7998	3.11	-0.17	no	none	no
HD170174	1	5345	3.04	0.35	no	red-giant	no
HD170200	41	SB2	none	no
HD170231	99	5398	3.55	0.23	no	red-giant	no
HD170270	1	4293	3.12	0.10	no	red-giant	no
HD170580	80	SB1	bCep	no
HD170625	1	9499	4.37	1.01	no	dSct	no
HD170699	110	SB1	dSct	no
HD170783	15	no	Be	yes
HD170973	16	no	a2CVn	no
HD171219	49	no	Be	yes
HD171427	1	5373	2.42	0.52	no	red-giant	no
HD171834	96	8491	4.73	0.50	no	gDor	no
HD172046	16	SB2	none	no
HD172910	1	SB1	SPB	no
HD174532	102	7861	3.71	0.16	no	dSct	no
HD174966	104	8958	4.17	0.86	SB1	HgMn	no
HD178169	25	SB2	none	no
HD178243	1	8647	4.33	0.33	no	none	no
HD178484	145	5017	3.23	0.36	no	red-giant	no
HD179079	261	5767	4.10	0.29	no	solar-like	no
HD179192	1	12937	3.76	-0.28	no	none	no
HD181907	116	5133	3.18	0.32	no	red-giant	no
HD184552	14	8887	4.12	0.88	no	dSct	no
HD186786	1	7928	3.77	0.20	no	dSct	no
HD188032	10	8451	4.66	0.31	no	gDor	no
HD188136	1	7206	3.95	-0.62	no	dSct	no
HD188224	1	7256	3.79	0.01	no	dSct	no
HD188520	1	7585	3.29	0.15	no	dSct	no
HD189631	49	7603	3.83	0.31	no	gDor	no
HD191301	1	8258	3.66	0.37	no	dSct	no
HD193084	1	no	none	no
HD194492	1	7333	3.57	0.17	no	dSct	no
HD195961	38	6634	2.30	0.39	no	dSct	no
HD196517	1	9509	4.73	1.02	no	dSct	no
HD196638	1	7043	2.86	-0.06	no	dSct	no
HD197451	3	7187	2.95	0.34	no	gDor	no
HD199124	1	8403	3.72	0.32	no	dSct	no
HD199434	2	6821	2.86	0.09	no	dSct	no
HD201985	2	7771	3.92	0.06	SB1	gDor	no
HD203699	1	no	Be	yes
HD203699	0	no	Be	yes
HD205879	6	11626	3.56	0.60	no	SPB	no
HD206379	1	7853	3.97	-0.02	no	dSct	no
HD206481	7	8870	4.79	0.71	no	gDor	no
HD206553	1	7816	3.73	0.12	no	dSct	no

Table A.1. continued.

Target name	N. spectra	T_{eff}	$\log g$	[Fe/H]	Binary	Variable type	H α emission
HD208664	1	7830	3.56	0.35	no	dSct	no
HD208999	1	6968	3.62	0.41	no	dSct	no
HD209775	2	8475	3.94	0.92	no	dSct	no
HD210111	1	8095	4.10	-0.70	no	dSct	no
HD213204	1	7918	4.00	0.18	no	dSct	no
HD213655	1	7034	3.16	0.14	no	dSct	no
HD214291	6	SB2	gDor	no
HD216113	1	8966	4.04	0.80	no	none	no
HD220978	1	8216	3.76	0.00	no	dSct	no
HD223065	89	9138	5.02	-0.07	no	dSct	no
HD224288	6	7385	3.79	0.38	no	gDor	no
HD224875	1	8189	3.41	0.30	no	dSct	no
HD261331	3	9140	4.14	0.91	no	dSct	no
HD261446	3	7543	3.21	0.28	no	dSct	no
HD269858	8	no	SDor	yes
HD290327	7	5987	5.02	0.32	no	none	no
HD290764	1	8117	4.13	-0.14	no	dSct	yes
Sun	21	5777	4.44	0.00	no	solar-like	no
V2129Oph	7	no	TTau	yes
V585Oph	1	no	red-giant	no